Mécanique & Industries 10, 365–376 (2009)
www.mecanique-industries.org
Mécanique & Industries

DOI: 10.1051/meca/2009070

Effect of manufacturing defects on the dynamic behaviour for an helical two-stage gear system

Lassâad Walha, Yassine Driss[a], Tahar Fakhfakh and Mohamed Haddar

Unit research of mechanical systems dynamics, National engineering school of Sfax, Tunisia

Received 11 March 2008, Accepted 6 August 2009

Abstract – The modelling of the dynamic behaviour of three-dimensional model of two-stage gear system is formulated for general helical gears location. The excitation is induced by the periodic variation of the mesh stiffnesses. This case describes the real working of the gearings. First, the modal analysis of the system is treated. Then, the calculation of the dynamic response is performed by a step-by-step time integration method (Newmark method). Finally, two types of manufacturing defects on the gears are introduced in the model: eccentricity and profile defect. An analysis of the effects of these defects on the gear system dynamic behaviour is then treated.

Key words: Helical two-stage gear / eccentricity /profile error

Résumé – Effets des défauts de fabrication sur le comportement dynamique d'une transmission par engrenage à deux étages à denture hélicoïdale. La modélisation du comportement dynamique d'un modèle spatial relative à une transmission par engrenage à deux étages à denture hélicoïdale est formulée pour une disposition générale des roues dans le carter. La principale source d'excitation est la variation périodique de la raideur d'engrènement. Dans une première étude une analyse modale est traitée. Ensuite le comportement dynamique est déterminé grâce à la méthode de résolution numérique pas à pas dans le temps (méthode de Newmark). Finalement, deux types de défauts de fabrication des roues sont introduits dans le modèle : défaut d'excentricité et défaut de profil. L'analyse des effets de ces défauts sur le comportement dynamique du système est étudiée.

Mots clés : Transmission à deux étages / denture hélicoïdale / défaut d'excentricité / défaut de profil

1 Introduction

Gearing is actually the best solution to transmit rotational motions and couple which has been offered numerous advantages [1]: it ensures a mechanical reliability and its mechanical efficiency is of the order of 0.96 to 0.99. But today, several applications inquire for the gearing transmissions to be more and more reliable, light and having long useful life that requires the control of the acoustic broadcast and the vibratory behaviour of these gearings [2].

The literature is rich by theoretical and experimental works achieved on the gearings. Several problems have treated on the one stage gear system [3, 4]. Yakhou [5] worked on the helical teeth in the gearboxes. He mentionned the different origins of the noises radiated by these boxes. He introduced in the model the casing and the rolling bearings. His work was validated by an experimental part. Perret-Liaudet [6] introduced some flexible shafts in his one stage gear model. To solve the dynamics response of the system, he used an iterative spectral method that permits to reduce the time of the calculation.

The works of research [6–14] included the different types of defects that may affect the gearings. Indeed, the researchers are interested in the gearing defects allowing them to be able to analyze the dynamic behaviour of the transmission in presence of these defects. Parker et al. [15] treated a plane problem of two-stage gear systems constituted by three toothed wheels without introducing neither the flexibility of the bearing nor the shaft one. They were interested in the problem of instabilities in these systems. However, the previous investigations have treated only models of two-stage gear systems with spur gear. In this paper, a three-dimensional model of two-stage gear systems in permanent working state is developed. Then, the numeric results concerning the dynamic response are obtained thanks to an algorithm of numerical integration (Newmark algorithm [8]). Finally, the cases of perfect and defected gearbox with two geometric defects are then studied.

[a] Corresponding author: drissyassine@yahoo.fr

Nomenclature

[C]	proportional damping matrix
E_{ptot}	potential energy coming from the misalignment
fe_i	mesh frequencies (Hz)
$\{F_0\}$	external force vector
h	mesh phasing
j	$j = 1$ to 3; number of the block
$k_{\phi j}$, $k_{\psi j}$	bending stiffness of the bearing j (N/m)
k_{xj}, k_{yj}, k_{zj}	traction-compression stiffness of the bearing j (N.m/rad)
$k_{\theta j}$	torsional stiffness of the shaft j (N/m)
$[\mathrm{K_s}]$	average stiffness matrix of the structure
$[\mathrm{K}(t)]$	gear mesh stiffness matrix
$[\mathrm{K_C}]$	mean matrix component
$[\mathrm{K_V}]$	time mesh stiffness varying matrix component with zero average
$\left[\tilde{\mathrm{K}}\right]$	global average stiffness matrix of the model
$L_{\max}$	maximal length of contact line (N/m)
$L_{\min}$	minimal length of contact line (N/m)
[M]	time independent system mass matrix
$\{q\}$	generalised coordinate's vector
$\{q_{\mathrm{S}}\}, \{q_{\mathrm{d}}\}$	static and dynamic components of the generalised coordinate's vector
Rb_{ij}	basic radius of the wheel i related to block j (m)
x_j, y_j, z_j	translational displacements of the bearing j (N/m)
Z_{ij}	teeth numbers of the gears (ij)
α_i	pressure angles (°)
β	helix angle (°)
χ	angle between the center lines which locates the second stage relatively to the first (°)
γ_i	angle that the line of the gear centers makes with the stationary axis (°)
δ_s	teeth deflections ($s = 1, 2$) (m)
ε_α	contact ratio
ε_β	overlap ratio

2 Model of the two-stage gear system

Two-stage gear system is composed of two trains of gearings. Every train links two blocks. So, the gear system has in totality three blocks ($j = 1$ to 3) [5,16]. Every block (j) is supported by flexible bearing the stiffness of which k_{xj}, k_{yj}, k_{zj}, $k_{\phi j}$ and $k_{\psi j}$ are the traction-compression and the bending stiffness [17]. Moreover, the shafts (j) are only submitted to the torsional motion and admit some torsional stiffness $k_{\theta j}$. The wheels 11 and 32 characterize respectively the motor side and the receiving machine side which inertias are I_{m} and I_{r} [18]. The other helical gears constitute the gearbox. The gear meshes are modelled by linear spring along the lines of action (Fig. 1). x_j, y_j and z_j are supposed the translational displacements of the bearing. The shaft lengths are considered of the same order of the teeth width. Moreover, it is assumed that the masses of shafts are negligible.

3 Mesh stiffness variation modelling

The meshes stiffness variations $k_1(t)$ and $k_2(t)$ are modelled by trapezoidal waves that depend on the features of the gearings [18]. It is proportional to the length of contact line. The basic length l' (Fig. 2), the contact ratio ε_α and the overlap ratio ε_β are defined by [18]:

$$l' = (P_b^2 + P_x^2)^{1/2}; \tag{1}$$

$$\varepsilon_\alpha = L/P_{b=A+a}; \tag{2}$$

$$\varepsilon_\beta = l'/P_x = B + b; (A, B : \text{real parts}, a, b : \text{decimal parts}) \tag{3}$$

The maximal length $L_{\max}$ and the minimal length $L_{\min}$ (Fig. 3) are defined as follows:

$$L_{\max} = (AB + Ab + aB + c)l'; \tag{4}$$

$$\text{if } (a+b) > 1 : L_{\min} = (AB + Ab + aB + (a + b - 1))l'; \tag{5}$$

$$\text{if } (a+b) < 1 : L_{\min} = (AB + Ab + aB)l'; \quad \text{With } c \text{ the smallest of } a \text{ and } b \tag{6}$$

$\varepsilon_{\alpha i}$ are the contact ratios ($i = 1, 2$). Mesh frequencies fe_i are related by the following relation [15]:

$$fe_2 = \frac{Z_{22}}{Z_{21}} fe_1 \tag{7}$$

Z_{21} and Z_{22} represent the teeth numbers of the gears (21) and (22). The term p_i represents "the initial phasing" for

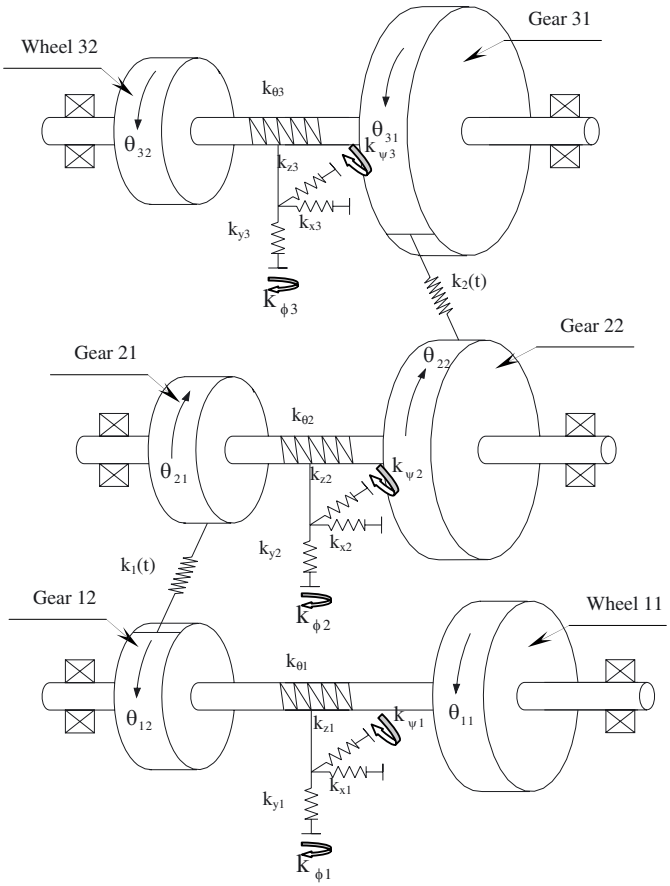

Fig. 1. Model of the two-stage gear system.

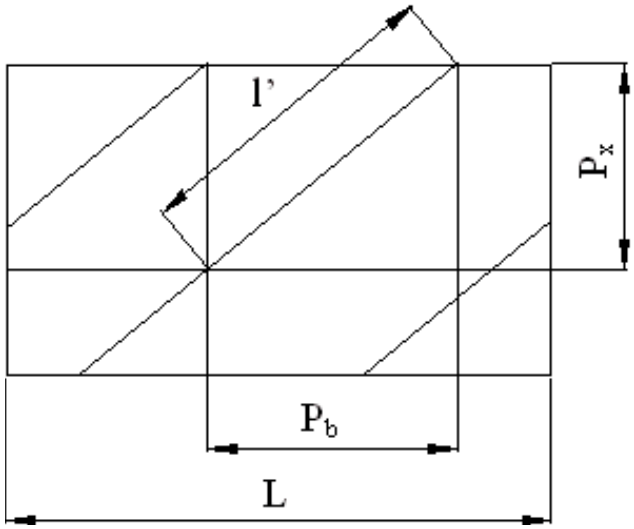

Fig. 2. Traces of the contact line in the action plan [18].

the mesh stiffness on the stage i. Mesh phasing h between the two mesh stiffness 1 and 2 (Fig. 9) is expressed by [15]:

$$h = \frac{\chi Z_{22}}{2\pi} \tag{8}$$

χ represents the angle between the lines of the centres and locates the second stage relatively to the first. To simplify

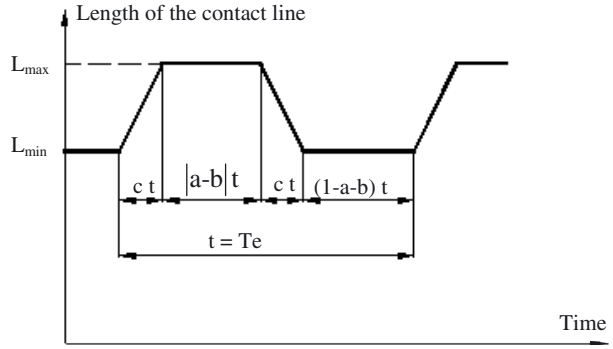

Fig. 3. Modelling of the mesh stiffness variation of the helical gear [18].

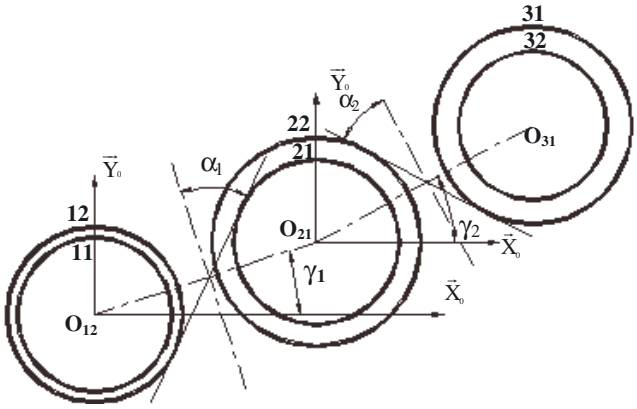

Fig. 4. Positions of the wheels of the helical two stage-gear system.

the problem, it is supposed that $\gamma_1 = 0°$ (Fig. 4), then χ is expressed by:

$$\chi = \pi - \gamma_2 \tag{9}$$

4 Equations of motion

The positions of the wheels of the helical two stage-gear system are represented by Figure 4. αi are the pressure angles. Every γi designates the angle that the line of the gear centers makes with the stationary axis $\left(O, \vec{X}_0\right)$.

4.1 Expression of the teeth deflections

The generalised coordinate's vector $\{q\}$ includes twenty-one degrees of freedom. Indeed, each block j has seven degrees of freedom: five degrees $(x_j, y_j, z_j, \phi_j, \psi_j)$ corresponding to the bearing j displacements (three translations and two rotations) and two degrees $(\theta_{1j}, \theta_{2j})$ corresponding to the wheels (1) and (2) of the shaft j (due to the above hypothesis):

$$\{q\} = \{x_1, y_1, z_1, x_2, y_2, z_2, x_3, y_3, z_3, \phi_1, \psi_1, \phi_2, \psi_2, \phi_3, \psi_3, \theta_{11}, \theta_{12}, \theta_{21}, \theta_{22}, \theta_{31}, \theta_{32}\} \tag{10}$$

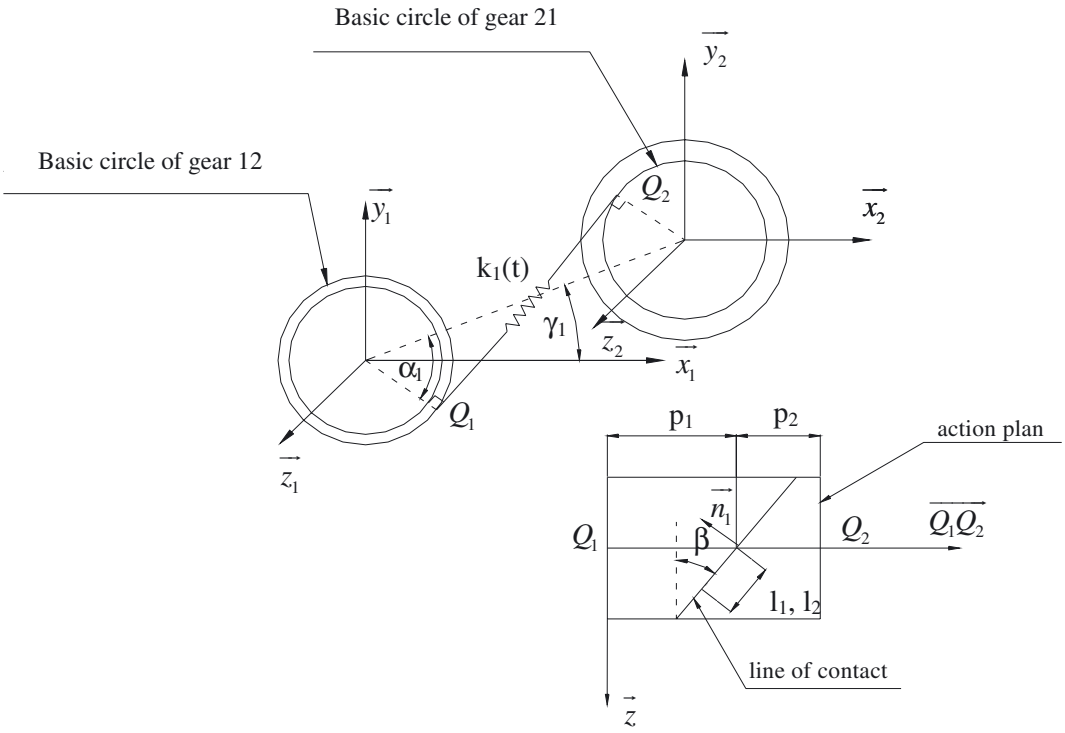

Fig. 5. Modelling of the connection between gear (12) and gear (21).

Table 1. Constants appearing in the expression of $\delta_1(l,t)$.

s_1	$\cos\beta\sin(\gamma_1-\alpha_1)$
s_2	$\cos\beta\cos(\gamma_1-\alpha_1)$
s_3	$\sin\beta$
s_4	$-l\cos^2\beta\cos(\gamma_1-\alpha_1)+\sin\beta(-Rb_{12}\sin(\alpha_1-\gamma_1)+\cos(\gamma_1-\alpha_1)(p_1-l\sin\beta))$
s_5	$-l\cos^2\beta\sin(\gamma_1-\alpha_1)-\sin\beta(Rb_{12}\cos(\alpha_1-\gamma_1)+\sin(\gamma_1-\alpha_1)(l\sin\beta-p_1))$
s_6	$Rb_{12}\cos\beta$
s_7	$l\cos^2\beta\cos(\gamma_1-\alpha_1)-\sin\beta(Rb_{21}\sin(\alpha_1-\gamma_1)-\cos(\gamma_1-\alpha_1)(p_2+l\sin\beta))$
s_8	$l\cos^2\beta\sin(\gamma_1-\alpha_1)+\sin\beta(-Rb_{21}\cos(\alpha_1-\gamma_1)+\sin(\gamma_1-\alpha_1)(p_2+l\sin\beta))$
s_9	$Rb_{21}\cos\beta$

The first teeth deflection $\delta_1(t)$ is written as follows (Fig. 5):

$$\delta_1(t) = L_{\delta 1}\{q\} \tag{11}$$

$$L_{\delta 1} = [-s_1\ s_2\ s_3\ s_1\ -s_2\ -s_3\ 0\ 0\ 0\ s_4\ s_5\ s_7\ s_8\ 0\ 0\ 0\ s_6\ s_9\ 0\ 0\ 0] \tag{12}$$

The constants s_i are given in Table 1. In this table, the distances p_1 and p_2 are defined by:

$$p_1 = Rb_{12}\,\mathrm{tg}\,\alpha_1 \quad ; \quad p_2 = Rb_{21}\,\mathrm{tg}\,\alpha_1 \tag{13}$$

Rb_{ij} is the basic radius of the wheel j related to block i.

The second teeth deflection $\delta_2(t)$ is supposed to be defined by the product of L by $\{q\}$ and written as follows (Fig. 6):

$$L_{\delta 2} = [0\ 0\ 0\ t_1\ -t_2\ t_3\ -t_1\ t_2\ -t_3\ 0\ 0\ t_4\ t_5\ t_7\ t_8\ 0\ 0\ 0\ t_6\ t_9\ 0] \tag{14}$$

The constants t_i are given in Table 2. In this table, the distances p_2' and p_3 are defined by:

$$p_3 = Rb_{22}\,\mathrm{tg}\,\alpha_2 \quad ; \quad p_4 = Rb_{31}\,\mathrm{tg}\,\alpha_2 \tag{15}$$

4.2 Matrix differential equation

Lagrange formalism leads to the set of differential equations governing the system motion:

$$[\mathrm{M}]\{\ddot{q}\} + [\mathrm{C}]\{\dot{q}\} + ([\mathrm{Ks}] + [\mathrm{K}(t)])\{q\} = \{\mathrm{F}_0\} \tag{16}$$

[M] represents the time independent system mass matrix. The average stiffness matrix of the structure is noted by [$\mathrm{K_s}$].

$$[K_S] = \begin{bmatrix} K_p & 0 \\ 0 & K_\theta \end{bmatrix} \tag{17}$$

[$\mathrm{K_p}$] can be written as follow:

$$[\mathrm{K_p}] = \mathrm{diag}(k_{x1}, k_{y1}, k_{z1}, k_{x2}, k_{y2}, k_{z2}, k_{x3}, k_{y3}, k_{z3}) \tag{18}$$

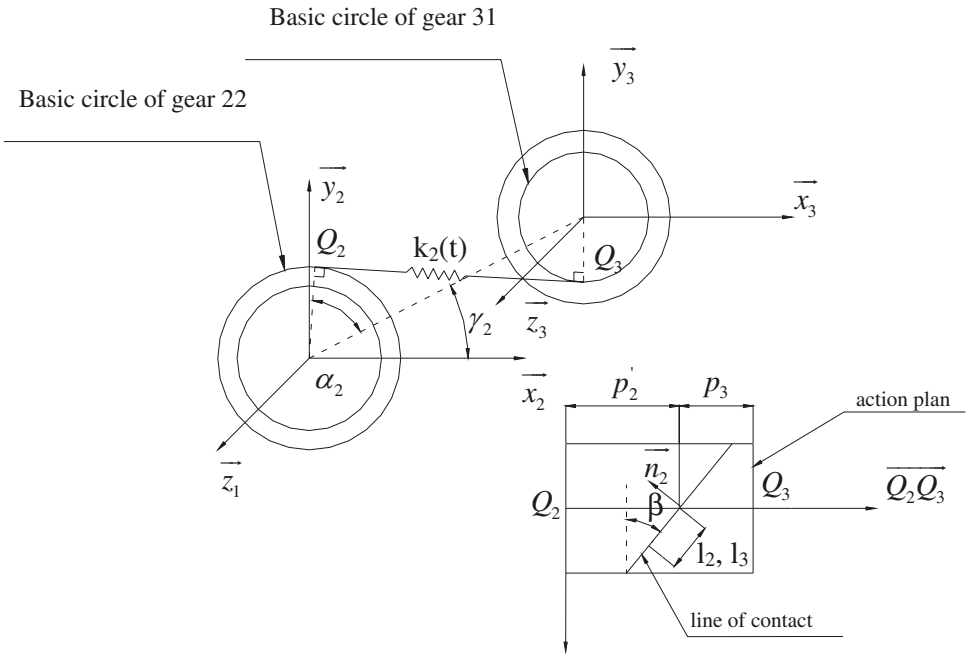

Fig. 6. Modelling of the connection between gear (22) and gear (31).

Table 2. Constants appearing in the expression of $\delta_2(l,t)$.

t_1	$\cos\beta\sin(\alpha_2+\gamma_2)$
t_2	$\cos\beta\cos(\alpha_2+\gamma_2)$
t_3	$\sin\beta$
t_4	$l\cos^2\beta\cos(\alpha_2+\gamma_2)+\sin\beta(Rb_{22}\sin(\alpha_2+\gamma_2)+\cos(\alpha_2+\gamma_2)(l\sin\beta-p_3))$
t_5	$l\cos^2\beta\sin(\alpha_2+\gamma_2)-\sin\beta(Rb_{22}\cos(\alpha_2+\gamma_2)+\sin(\alpha_2+\gamma_2)(p_3-l\sin\beta))$
t_6	$-Rb_{22}\cos\beta$
t_7	$-l\cos^2\beta\cos(\alpha_2+\gamma_2)-\sin\beta(-Rb_{31}\sin(\alpha_2+\gamma_2)+\cos(\alpha_2+\gamma_2)(l\sin\beta+p_4))$
t_8	$-l\cos^2\beta\sin(\alpha_2+\gamma_2)+\sin\beta(-Rb_{31}\cos(\alpha_2+\gamma_2)-\sin(\alpha_2+\gamma_2)(p_4+l\sin\beta))$
t_9	$-Rb_{31}\cos\beta$

$[\mathrm{K}_\theta]$ is composed by shafts stiffness and it is expressed by:

$$[K_\theta] = \begin{bmatrix} k_{\phi1} & 0 & 0 & 0 & 0 & 0 & 0 & 0 & 0 & 0 & 0 & 0 \\ 0 & k_{\psi1} & 0 & 0 & 0 & 0 & 0 & 0 & 0 & 0 & 0 & 0 \\ 0 & 0 & k_{\phi2} & 0 & 0 & 0 & 0 & 0 & 0 & 0 & 0 & 0 \\ 0 & 0 & 0 & k_{\psi2} & 0 & 0 & 0 & 0 & 0 & 0 & 0 & 0 \\ 0 & 0 & 0 & 0 & k_{\phi3} & 0 & 0 & 0 & 0 & 0 & 0 & 0 \\ 0 & 0 & 0 & 0 & 0 & k_{\psi3} & 0 & 0 & 0 & 0 & 0 & 0 \\ 0 & 0 & 0 & 0 & 0 & 0 & k_{\theta1} & -k_{\theta1} & 0 & 0 & 0 & 0 \\ 0 & 0 & 0 & 0 & 0 & 0 & -k_{\theta1} & k_{\theta1} & 0 & 0 & 0 & 0 \\ 0 & 0 & 0 & 0 & 0 & 0 & 0 & 0 & k_{\theta2} & -k_{\theta2} & 0 & 0 \\ 0 & 0 & 0 & 0 & 0 & 0 & 0 & 0 & -k_{\theta2} & k_{\theta2} & 0 & 0 \\ 0 & 0 & 0 & 0 & 0 & 0 & 0 & 0 & 0 & 0 & k_{\theta3} & -k_{\theta3} \\ 0 & 0 & 0 & 0 & 0 & 0 & 0 & 0 & 0 & 0 & -k_{\theta3} & k_{\theta3} \end{bmatrix} \quad (19)$$

$[\mathrm{K}(t)]$ is the gearmesh stiffness matrix. It is a time varying matrix and can be expressed by:

$$[\mathrm{K}(t)] = (\mathrm{L}_{\delta1})^{\mathrm{T}}\,\mathrm{L}_{\delta1}k_1(t) + (\mathrm{L}_{\delta2})^{\mathrm{T}}\,\mathrm{L}_{\delta2}k_2(t) \quad (20)$$

$k_1(t)$ ant $k_2(t)$ are the time varying mesh stiffness functions.

$[\mathrm{K}(t)]$ can then be written as:

$$[\mathrm{K}(t)] = [\mathrm{K_C}] + [\mathrm{K_V}(t)] \quad (21)$$

where $[\mathrm{K_C}]$ is the mean matrix component, $[\mathrm{K_V}(t)]$ is the time varying matrix component with zero average.

It is noted that $\left[\tilde{\mathrm{K}}\right]$ is the global average stiffness matrix of the model. This time independent matrix is expressed by:

$$\left[\tilde{\mathrm{K}}\right] = [\mathrm{K_S}] + [\mathrm{K_C}] \quad (22)$$

$[\mathrm{K_S}]$ is defined in equation (17).

The vector $\{q\}$ can be decomposed in static and dynamic components vector as:

$$\{q\} = \{q_\mathrm{S}\} + \{q_\mathrm{d}\} \quad (23)$$

The pseudo static component $\{q_\mathrm{S}\}$ is introduced by:

$$\left[\tilde{\mathrm{K}}\right]\{q_\mathrm{S}\} = \{F_0\} \quad (24)$$

Table 3. System parameters.

Material :42CrMo4	$\rho = 7860$ Kg.m^{-3}	
Motor characteristics	Motor torque	$Cm = 1000$ N.m
	Motor inertia	$Im = 3.5 \times 10^{-4}$ Kg.m^2
	Motor speed	$Nm = 1500$ rpm
Receiving characteristics	Receiving torque	$Cr = -2888$ N.m
	Receiving inertia	$Ir = 6.5 \times 10^{-4}$ Kg.m^2
Bearing stiffness	$k_{xi} = 10^8$ N.m^{-1} ; $k_{yi} = 10^8$ N.m^{-1} ; $k_{zi} = 10^8$ N.m^{-1}	
Shafts torsional stiffness	$k_{\theta i} = 3 \times 10^5$(N.m^{-1})/rad	
	First gearmesh	Second gearmesh
Pressure angle	$\alpha_n = 20°$	
Helix angle	$\beta = 20°$	
Teeth module	$m_n = 4 \times 10^{-3}$ m	
Teeth number	$Z12 = 18$; $Z21 = 26$	$Z22 = 20$; $Z31 = 40$
Average mesh stiffness	$k_{\text{moy}} = 410^8$ N.m^{-1}	$k_{\text{moy}} = 410^8$ N.m^{-1}
Contact ratio	$\varepsilon_{\alpha 1} = 2.7$	$\varepsilon_{\alpha 2} = 3.7$
Covering ratio	$\varepsilon_{\beta 1} = 1.09$	$\varepsilon_{\beta 2} = 1.09$
Teeth width	$b = 35 \times 10^{-3}$ m	

Where the external force vector $\{F_0\}$ can be written as:

$$\{F_0\} = \{0,0,0,0,0,0,0,0,0,0,0,0,0,0,0,Cm, 0,0,0,0,-Cr\}^{\mathrm{T}} \quad (25)$$

In this context, a proportional damping is considered and can be expressed by: [19]

$$[\mathrm{C}] = \lambda\,[\mathrm{M}] + \mu\left[\tilde{\mathrm{K}}\right] \quad (26)$$

where λ and μ are the damping constants defined by:

$$\lambda = \mu = 0.03 \quad (27)$$

The matrix differential equation governing the dynamic component behaviour will then be written as:

$$[\mathrm{M}]\{\ddot{q}_{\mathrm{d}}\} + [\mathrm{C}]\{\dot{q}_{\mathrm{d}}\} + ([\mathrm{K_S}] + [\mathrm{K}(t)])\{q_{\mathrm{d}}\} = -[\mathrm{K_V}(t)]\{q_{\mathrm{s}}\} \quad (28)$$

5 Modal analysis

Table 3 regroups the technological and dimensional features of the two-stage gear system. The frequencies and modal deflections are determined while assimilating the matrix stiffness of the model to the average matrix noted by $[\tilde{\mathrm{K}}]$. Table 4 regroups the first natural frequencies of the system for three locations of the wheels. The presence of null frequency characterizing of rigid body motion is noticed. Also, it is noted that the optimal position, which optimizes the conception of the two-stage gear system, is defined by $\chi = 135°$.

Figures 7 and 8 represent some eigen modes of the wheels for the three cases of wheels location. The dashed lines indicate the initial wheels positions. The first mode has purely rotational motion and characterizes the rigid body motion. The sixth mode is a combined motion of translation and rotation. The ninth mode is a mode of pure translational motion.

Table 4. Eigen frequencies of the model.

Frequency	$\chi = 180°$ $h = 0$	$\chi = 135°$ $h = 0.5$	$\chi = 80°$ $h = 0.44$
f_1	0	0	0
f_2	1660	1680	1720
$f_3 = f_4$	2080		
f_5	2270	2300	2380
f_6	2530	2490	2440
f_7	2610		
f_8	3690	3680	3620
$f_9 = f_{10}$	4160		
f_{11}	6170	6120	5960

According to the Table 4, it is noticed that:

- the eigen frequencies f_3 and f_4 (respectively f_9 and f_{10}) are equal for every wheels positions. Moreover, it is noted that the eigen modes associated to these frequencies present only translational displacements at the third bearing (respectively at the first one);
- the frequency f_7 is independent of the position of the wheels.

6 Dynamic response for two-stage gear system without defects

The calculation of the dynamic response is performed by a step-by-step time integration method (Newmark method). The step of integration is equal to 10^{-5} s. For the two-stage gear system without defects, the main

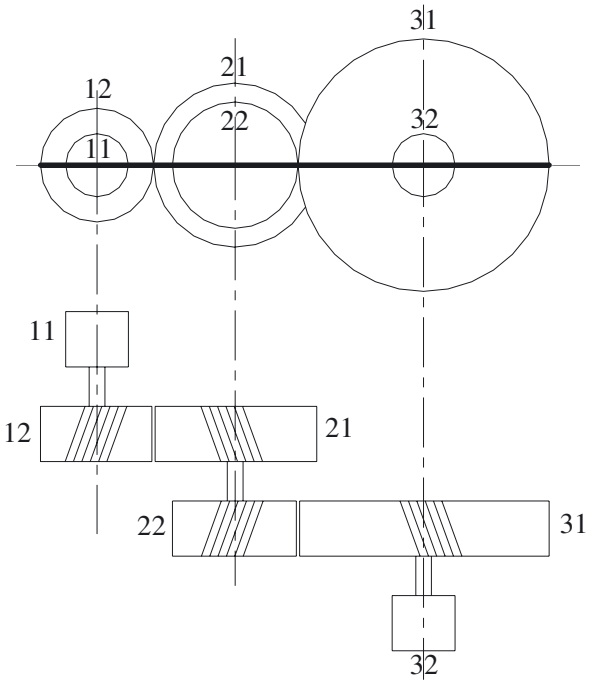

Reference position

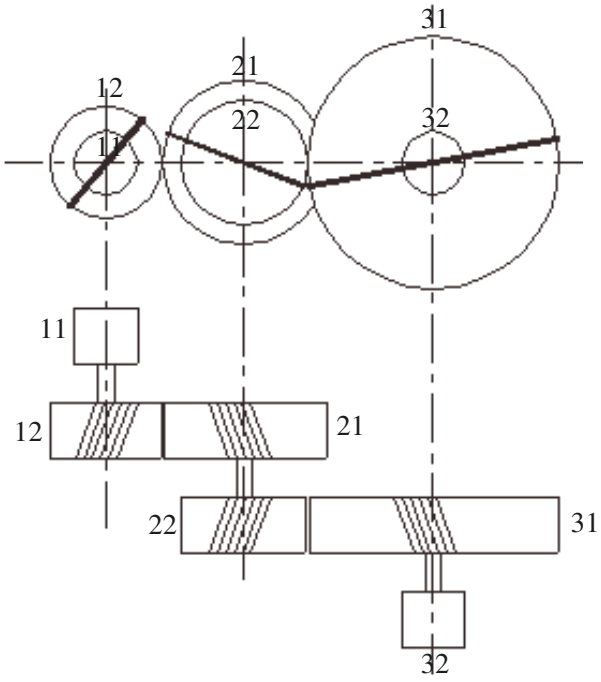

First mode (Rigid body motion)

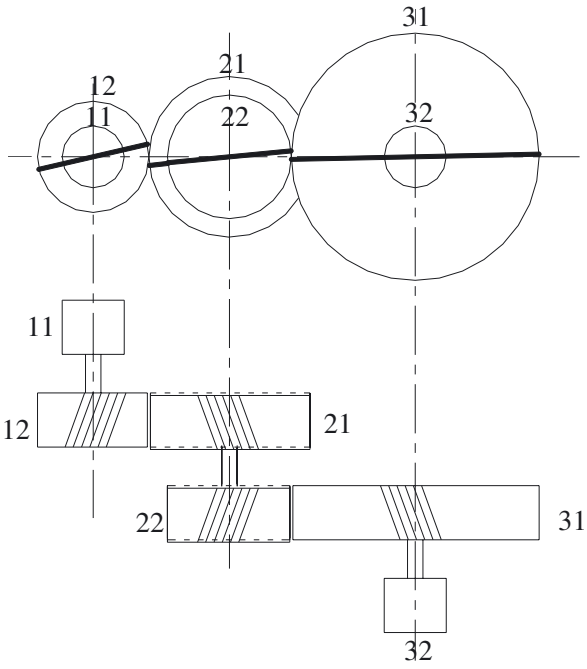

Sixth mode ($f = 2530$ Hz)

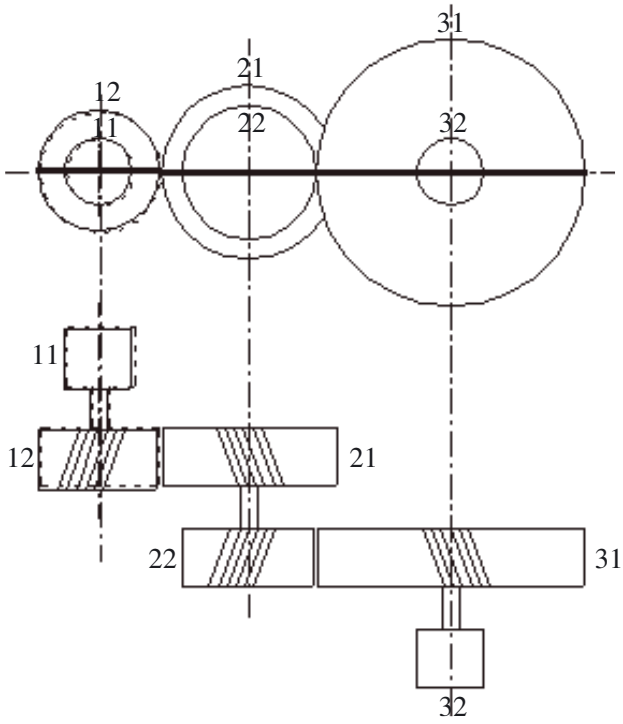

Ninth mode ($f = 4160$ Hz)

Fig. 7. Typical vibration for the three types of modes for $\chi = 180°$.

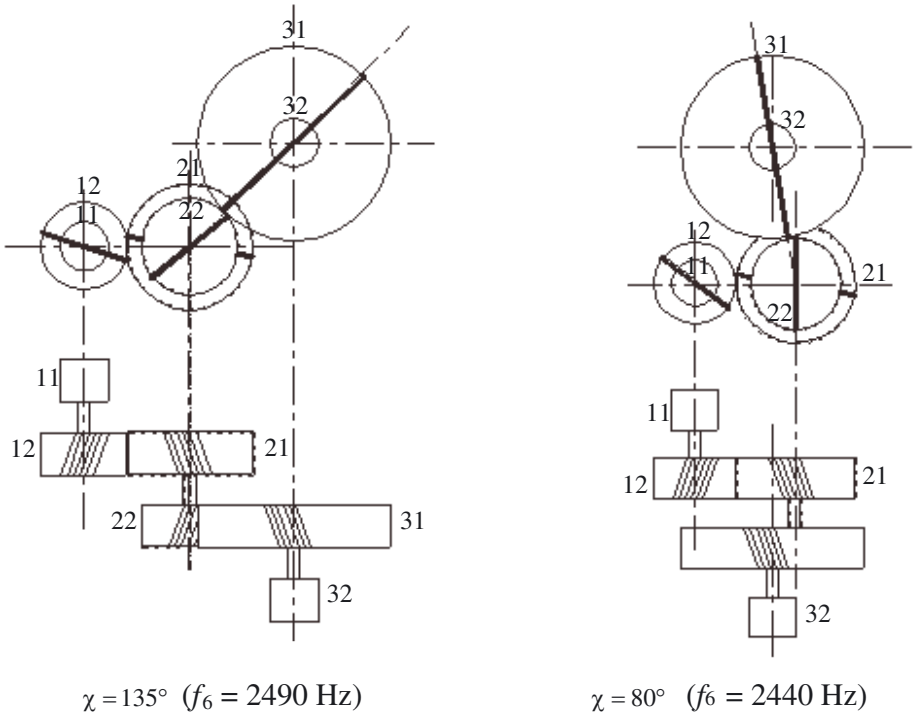

Fig. 8. Typical vibration for the Sixth mode.

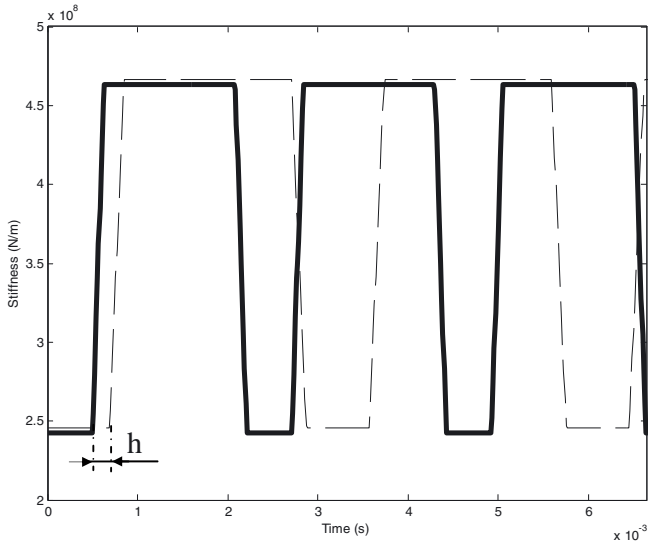

Fig. 9. Modelling of two mesh stiffness variation (–: $k_1(t)$; –:$k_2(t)$).

sources of excitation are the two mesh stiffness variations represented by Figure 9.

Figure 10 represents the frequency response of translational displacements resulting on the first bearing. It is clearly noticed the presence of several peaks in every signal. These peaks correspond to the two mesh frequencies $fe_1 = 450$ Hz and $fe_2 = 346$ Hz with their harmonics and other combined frequencies such as $fe_1 - fe_2$ and $fe_1 + fe_2$. The position which is defined by $\chi = 135°$, leads to the reduction of the gear system vibratory level.

7 Modelling of the defects

Most gearboxes include inherent defects following their manufacture. These defects may increase while working. They are essentially:

- errors of tooth: perfectly conjugated deviations of a profile of tooth, caused by imperfections of manufacture, or by a modification of profile;
- errors of manufacturing: as the eccentricity errors...

In this paper we try to approach two defects while supposing that they are the more met in the practice.

7.1 Modelling of the eccentricity defect

The transmission is now supposed having an eccentricity on gear (12). The eccentricity expresses the distance between the theoretical and the real rotational axis (Fig. 11) belonging to the first train of the two-stage gear system. O_{12} and G_{12} represent respectively the rotational and geometric centres of the gear (12). The eccentricity defect is defined by the parameter e_{12}, which represents the distance between the axis, and by a phase λ_{12} to specify the initial angular position.

An eccentricity defect causes teeth deflection on their own line of action. The deflection $\delta_1(t)$ is then added with a transmission error $e_{12}(t)$ defined by:

$$e_{12}(t) = e_{12}\sin(2\pi f_d - \lambda_{12} - \alpha_1) \qquad (29)$$

f_d is the frequency of defect. In our case, $f_d = f_1$.

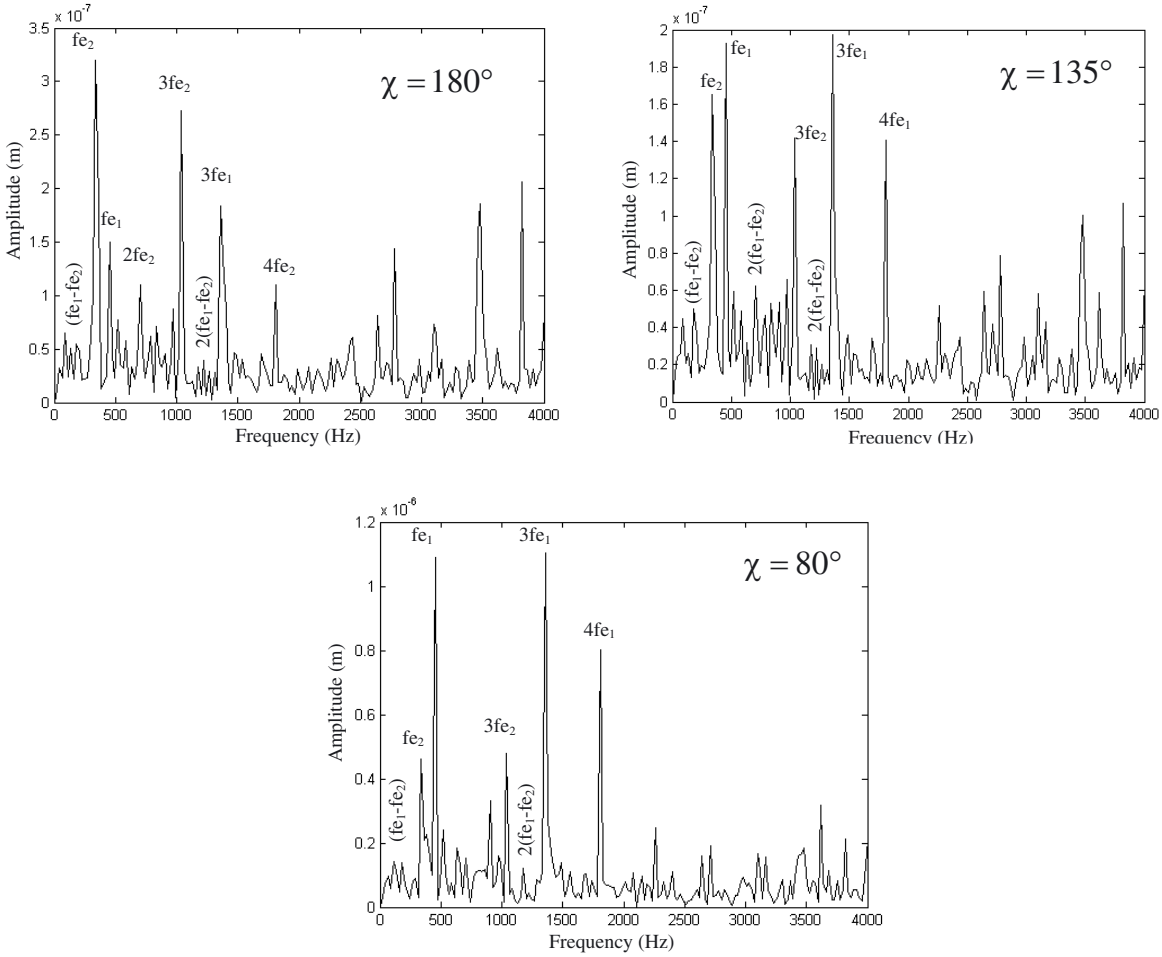

Fig. 10. Frequency dynamic responses of translational displacement resulting on the first bearing without defects.

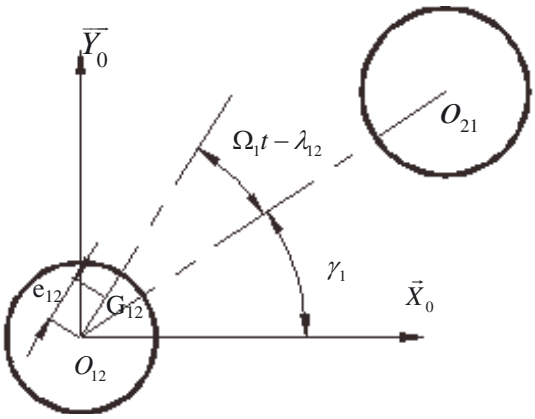

Fig. 11. Eccentricity defect.

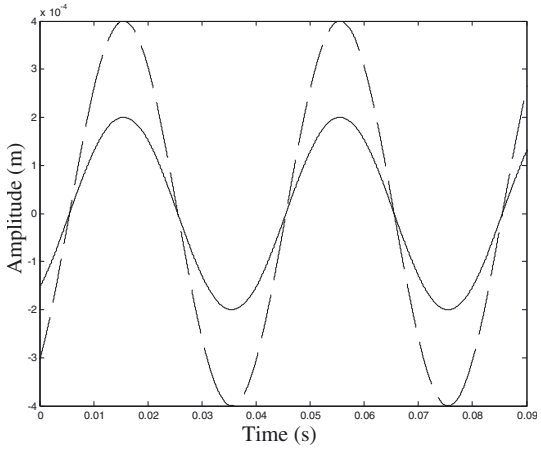

Fig. 12. Transmission error signal of the eccentricity defect ($-e_{12} = 200$ μm ,$-e_{12} = 400$ μm).

f_1 represents the frequency of rotation of the gear (12). Figure 12 shows the transmission error signal for two eccentricity amplitude defects. To analyze the real consequences of the defect on the dynamic behaviour of the model ($\chi = 135°$), two values of eccentricity are studied: $e_{12} = 200$ μm and $e_{12} = 400$ μm.

The potential energy due to the eccentricity defect can be written as:

$$E_{\text{ptot}} = \frac{1}{2} k_1(t) \left\{ e_{12}^2(t) + 2\delta_1(t) e_{12}(t) \right\} \qquad (30)$$

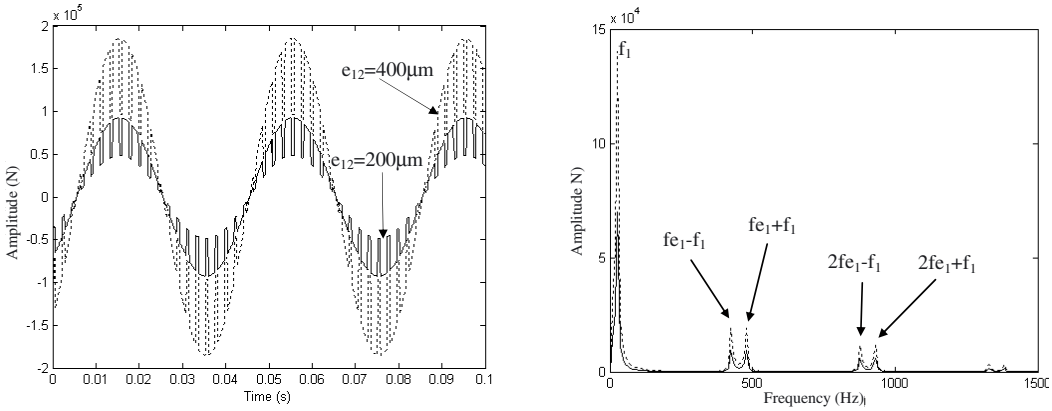

Fig. 13. Time and spectrum varying external force due to the eccentricity defect.

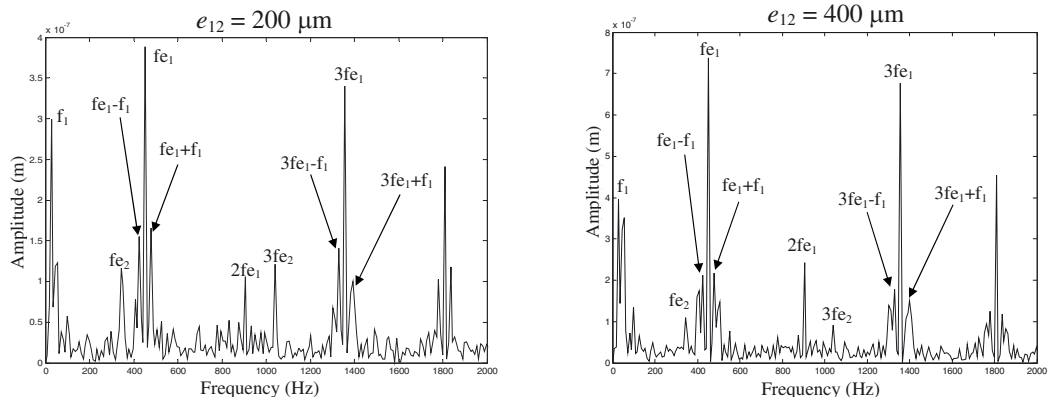

Fig. 14. Frequency dynamic response of the first bearing for eccentricity defect.

Then, the effect of the eccentricity defect can be expressed by the external force $\{F_{\text{pex}}(t)\}$ given by:

$$\{F_{\text{pex}}(t)\} = k_1(t)e_{12}(t)\{-s_1, s_2, s_3, s_1, -s_2, -s_3, 0, 0, 0, s_4, s_5, s_7, s_8, 0, 0, 0, s_6, s_9, 0, 0, 0\}^{\text{T}} \quad (31)$$

Figure 13 shows the time and the spectrum varying external force due to the eccentricity defect. The spectrum signal represents several peaks due to the modulating phenomenon resulting from eccentricity defect and mesh variation ($mfe_1 \pm nf_1$).

Figure 14 represents the dynamic displacement response spectrum of the first bearing for eccentricity defect.

The responses are characterized by the appearance of sidebands around the first mesh frequency ($fe_1 = 450$ Hz) and of its first harmonics. The appearance of a new peak besides the signal is noticed, this peak corresponds to the defect frequency ($f_1 = 25$ Hz). The modulation amplitude will be more and more amplified when the value of eccentricity is raised. This result is translated in the spectrum by the amplitudes amplification of the sidebands that surround the mesh frequency. The second mesh frequency ($fe_2 = 346$ Hz) will not be affected by the defect for any value of eccentricity.

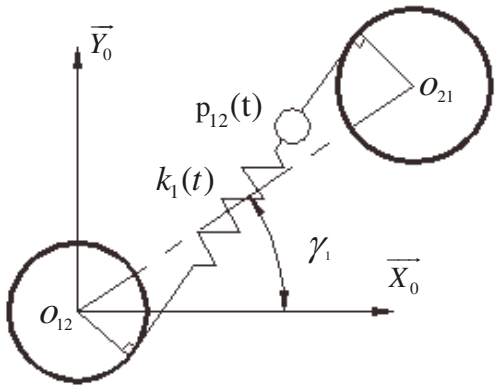

Fig. 15. Profile error modelling.

7.2 Effect of a profile error on the dynamic response

Profile errors result in imperfections on the geometry of the teeth. It is characterized by a shape deviation between the real profile and the theoretical profile of the tooth.

A profile error constitutes a source of important excitation in gearboxes. For similar teeth profiles error, these excitations are periodic of fundamental frequency equal to the mesh frequency corresponding to the wheel affected by this error.

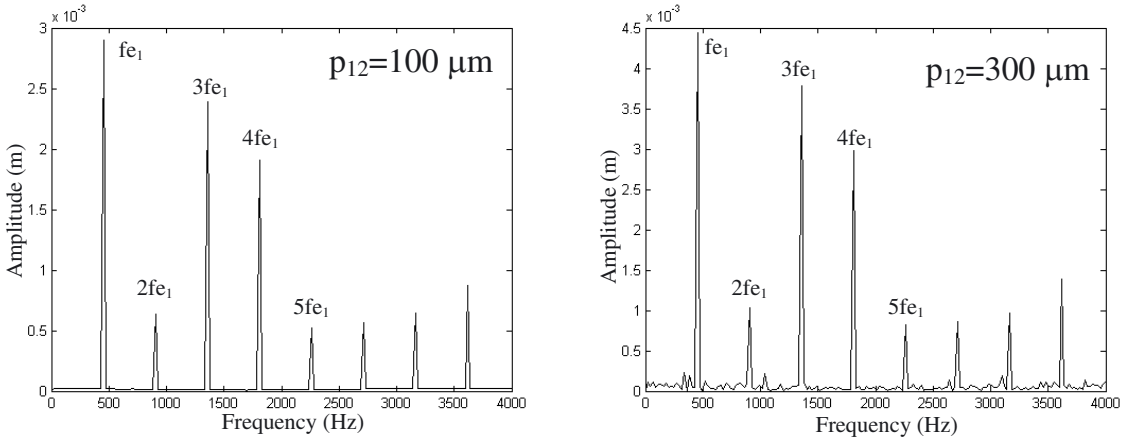

Fig. 16. Frequency responses of the first bearing with profile error ($\chi = 135°$).

As it is presented in the Figure 15, the defect of profile error is introduced by the addition of a displacement type term $p(t)$ to the tooth deflection on the line of action. This error is supposed identical on all teeth for the gear (12).

Its variation is assimilated by:

$$p_{12}(t) = p_{12} + \sum_{n=1}^{+\infty} p_{12}\, \sin(2\,\pi\, n\, fe_1\, t) \tag{32}$$

p_{12} and fe_1 represent respectively the profile error value and the first mesh frequency.

The profile error leads to a new external excitation expressed by:

$$\{F_{pp}(t)\} = k_1(t)\, \frac{\partial \delta_1(t)}{\partial q_i}\, p_{12}(t) \tag{33}$$

$$\{F_{pp}(t)\} = k_1(t) p_{12}(t) \{-s_1, s_2, s_3, s_1, -s_2, -s_3, 0, 0, 0, s_4, s_5, s_7, s_8, 0, 0, 0, s_6, s_9, 0, 0, 0\}^{\mathrm{T}} \tag{34}$$

The profile error will amplify the amplitude of the translational displacements on the three bearings. This result is clear in the Figure 16.

8 Conclusion

In this paper, the helical two-stage gear system was modelled by twenty-one degrees of freedom system with a time varying stiffness matrix. In the first time, the dynamic behaviour of the two-stage gear system without defects was made. A step-by-step time integration method (Newmark algorithm) was used to obtain this dynamic behaviour. The frequency dynamic response shows the domination of the peaks corresponding to the mesh frequencies. The dynamic response fluctuations are minimum for the second wheels location ($\chi = 135°$) that permits to reduce the gearbox size.

The helical two-stage gear system behaviour is affected by manufacturing defects. An amplitude modulation occurs when an eccentricity defect is introduced. This defect produced sidebands around the affected gearmesh frequency and its first harmonics.

A profile error increases the vibratory level. These surveys allow getting an idea on the characterisation of the dynamic response of the helical two-stage gear system affected by manufacturing defects.

References

[1] G.W. Blankenship, R. Singh, Dynamic force transmissibility in helical gear pairs, Mechanism and Machine Theory 29 (2000) 212–228

[2] C. Bard, Modélisation du comportement dynamique des transmissions par engrenages, thèse de doctorat, Institut National des Sciences Appliquées de Lyon, INSAL 0031, 1995

[3] P. Velex, M. Ajmi, On the modelling of excitations in geared systems by transmission errors, J. Sound Vib., 290 (2006) 882–909

[4] P. Velex, M. Ajmi, Dynamic tooth loads and quasi-static transmission errors in helical gears – Approximate dynamic factor formulae, Mechanism and Machine Theory 42 (2007) 1512–1526

[5] K. Yakhou, Validation expérimentale d'un modèle dynamique globale de boîte de vitesses automobile, Thèse de l'Institut National des Sciences Appliquées de Lyon, 2002

[6] Perret-Liaudet, Étude des mécanismes de transfert entre l'erreur de transmission et la réponse dynamique des boîtes de vitesses d'automobile, Thèse de l'École Centrale de Lyon, 1992

[7] F. Chaari, T. Fakhfakh, R. Hbaieb, J. Louati, M. Haddar, Influence of manufacturing errors on the dynamics behavior of planetary gears, International Journal of Advanced Manufacturing Technology 27 (2005) 738–746

[8] G. Dhatt, G. Touzot, Une présentation de la méthode des éléments finis, edition Maloine, 1984

[9] M. Haddar, M. Ben Amar, W. Gafsi, A. Maalej, Analyse du comportement dynamique et tribologique d'une transmission à engrenages droits en présence d'un défaut de parallélisme, 3e journées de mécanique et ingénierie, Sfax, Tunisie, 2000

[10] R. Hbaieb, F. Chaari, T. Fakhfakh, M. Haddar, Influence of eccentricity, profile error and tooth pitting on helical planetary gear vibration, Machine Dynamics Problems, 29 (2005) 5–32

[11] M. Lebold, K. McClintic, R. Cambell, C. Byington, K. Maynard, Review of vibration analysis methods for gearbox diagnostics and prognostics. Proceedings of the 54th Meeting of the Society for Machinery Failure Prevention Technology, Virginia Beach, 2000

[12] G. Litak, M.I. Friswell, Vibrations in gear systems, Chaos, Solitons & Fractals 16 (2003) 145–150

[13] A.J. Miller, A new wavelet basis for the decomposition of gear motion error signals and its application to gearbox diagnostics, Thèse de l'université de l'état de Pennsylvanie, 1999

[14] K.P. Maynard, Interstitial processing: the application of noise processing gear fault detection. Proceedings of the international conference on Condition monitoring, University of Wales Swansea, UK, 1999, pp. 77-86

[15] G.R. Parker, J. Lin, Mesh Stiffness Variation Instabilities in Two–stage Gear Systems, Journal of vibration and acoustics, 124 (2002)

[16] L. Walha, J. Louati, T. Fakhfakh, M. Haddar, Effects of eccentricity defect and tooth crack on two-stage gear system behaviour, International Journal of Engineering Simulation 6 (2005) 17–24

[17] T. Eritenel, R.G. Parker, Modal properties of three-dimensional helical planetary gears, J. Sound Vib., In Press, Corrected Proof, Available online 10 April 2009

[18] M. Maatar, Contribution à l'analyse du comportement dynamique de réducteurs à engrenages simple étage, Influence des écarts de forme et des défauts de montage, Thèse de l'Institut National des Sciences Appliquées de Lyon, 1995

[19] R. Bigret, J.L. Freon, Diagnostic, maintenance, disponibilité des machines tournantes, edition Masson, 1995